

and B^- denote the fields at the forward and trailing edge of the plasma, this condition is

$$B^+ + B^- = 2B_0 \quad (6)$$

Combining Eqs. (2-5) so as to eliminate either B_z or J_y and solving subject to the boundary condition (6) then results in

$$B_z = B_0 K_y + \frac{2B_0(1-K_y)}{(1+e^{Rm})} e^{Rmx/a} \quad (7)$$

and

$$J_y = -\frac{2B_0\sigma U_x(1-K_y) \cdot e^{Rmx/a}}{(1+e^{Rm})} \quad (8)$$

where

$$Rm = \mu_0\sigma U_x a \quad (9)$$

is the magnetic Reynolds number for the given geometry.

The local power density supported by the plasma is $P = \mathbf{J} \cdot \mathbf{E} = J_y E_y$. The total power delivered to the load is the negative integral of this quantity over the region of the plasma. Using Eqs. (2) and (8) in this integral, we obtain

$$P_t/A = 4 \left(\frac{B_0^2}{2\mu_0} \right) U_x K_y (1-K_y) \tanh \left(\frac{Rm}{2} \right) \quad (10)$$

This expression can be thought of as the equivalent to the low magnetic Reynolds number expression given by

$$(P_t/A)_{\text{low } Rm} = (B_0^2/\mu_0) U_x K_y (1-K_y) Rm \quad (11)$$

Equation (11) is familiar to many² and is used for order-of-magnitude calculations. Great care must be exercised in the use of Eq. (10) because of the approximations involved in its derivation. These approximations include the basic statements of the dimensionality of the MHD problem, i.e., the neglect of components other than $\mathbf{U} = (U_x, 0, 0)$, $\mathbf{B} = (0, 0, B_z)$, $\mathbf{J} = (0, J_y, 0)$, $\mathbf{E} = (0, E_y, 0)$ for the various vector quantities, the form of the Maxwell equations used, and the uniformity of the various quantities or the parameters $\sigma, U_x, E_y, B_0, J_y, K_y$ as well as the sharpness of the boundary conditions.

In general, other vector components of the fields and the fluid dynamic parameters will exist and the quantities $\sigma, U_x, B_0, K_y, E_y$, and B_z will vary with all three coordinates, giving rise under some conditions to internal circulating eddy currents.³ Thus, multidimensional computations are required for more detailed design analyses. Also, the conductivity is generally a tensor and the load may vary with x in the case of multielectrode generators and all the variables may vary with time, further adding to the complications.

Note that since $\tanh(Rm/2) \rightarrow 1$ as $Rm \rightarrow \infty$, the power obtained from a high magnetic Reynolds number device (e.g., one with very high conductivity) will reach the limit

$$P_t/A = 4(B_0^2/2\mu_0) U_x K_y (1-K_y) \quad (12)$$

and using the load-matching condition $K_y = 1/2$ we obtain for the maximum power from an MHD generator at high magnetic Reynolds numbers

$$(P_t/A)_{\text{max}} = (B_0^2/2\mu_0) U_x \quad (13)$$

Note that, since already at $Rm = 3$, $\tanh(Rm/2) > 0.9$, for $U = 10^4$ m/s and $a = 1$ m, we obtain $\sigma = 239$ mho/m. Therefore, there is an optimum conductivity for each pulsed MHD generator given by $\sigma \approx 3/(\mu_0 U a)$. This expression can be derived by reasoning that operation at a higher magnetic

Reynolds number is not required, especially since other losses or costs can only increase as Rm is increased. A higher conductivity is not necessary.

Note that Eq. (13) can be derived intuitively in a couple of ways (these results date from 1961 ± 1):

1) The magnetic pressure acting on the plasma in a region of magnetic field B_0 is $B_0^2/2\mu_0$. This is the force per unit area F/A acting to contain the plasma in the limit of very high magnetic Reynolds number and, therefore,

$$F/A = (B_0^2/2\mu_0) \quad (14)$$

The power that is produced by this plasma if it moves at a velocity U_x is therefore

$$U_x \cdot F/A = P_t/A = (B_0^2/2\mu_0) U_x \quad (15)$$

2) The energy contained in a magnetic field per unit volume is $B_0^2/2\mu_0$. At high magnetic Reynolds number a plasma sweeps out the magnetic field. The power removed per unit time associated with a one-dimensional sweep-out of the magnetic field by a plasma from region a will be

$$\text{Power}/wh = P_t/A = (B_0^2/2\mu_0) U_x \quad (16)$$

It is now appropriate to note that Eqs. (10) and (11) both approach zero as $Rm \rightarrow 0$. In other words, the power to the load vanishes as $Rm \rightarrow 0$. All other expressions are similarly well-behaved.

Acknowledgments

This work was supported under Contract F49620-83-C-0115, U.S. Air Force Office of Scientific Research, Directorate of Physical and Geophysical Sciences, Capt. Henry Pugh, Jr., Program Manager. The authors wish to acknowledge the help they have received from Dr. David A. Oliver in the form of many fruitful and enlightening discussions.

References

- ¹Demetriades, S. T., "Magnetohydrodynamic Orbit Control for Satellites," *Electrical Engineering*, Vol. 79, Dec. 1960, pp. 987-995.
- ²Rosa, R. J., *Magnetohydrodynamic Energy Conversion*, McGraw-Hill Book Co., New York, 1968.
- ³Oliver, D. A., Swean, T. F., Markham, D. M., Maxwell, C. D., and Demetriades, S. T., "High Magnetic Reynolds Number and Strong Interaction Phenomena in MHD Channel Flow," *Proceedings of the Seventh International Conference on MHD Electrical Power Generation*, Massachusetts Institute of Technology, Cambridge, Vol. II, 1980, p. 565.

Freestream Turbulence Effects on Turbulent Boundary Layers in an Adverse Pressure Gradient

R. L. Evans*

The University of British Columbia
Vancouver, Canada

Nomenclature

- C = constant in the law of the wall
 K = von Kármán constant
 Tu = turbulence intensity, $Tu = \bar{u}/U_\infty$

Received June 2, 1984; revision received Oct. 16, 1984. Copyright © American Institute of Aeronautics and Astronautics, Inc., 1985. All rights reserved.

*Associate Professor, Department of Mechanical Engineering.

- U = boundary-layer mean velocity
 U_∞ = freestream velocity
 u_τ = friction velocity, $u_\tau = \sqrt{\tau_w/\rho}$
 \tilde{u} = rms turbulence velocity
 w = Coles' wake function
 X/C = fraction of blade chord
 y = coordinate perpendicular to blade surface
 δ = boundary-layer thickness
 Π = parameter in Coles' law of the wake
 ρ = fluid density
 τ_w = wall shear stress

Introduction

FREESTREAM turbulence is known to significantly affect the development of turbulent boundary layers. Several studies (see, e.g., Refs. 1-6) have detailed the effects of freestream turbulence intensity on the boundary-layer integral parameters such as momentum thickness and skin friction. In a detailed study, Hancock⁷ has examined the effects of scale as well as intensity for a range of length scales of the same order of magnitude as the boundary-layer thickness. In general, Hancock found that the effects of freestream turbulence decrease with increasing length scale, at least in the range studied.

All of the previously mentioned studies have been carried out with boundary layers developing in a zero pressure gradient. The designer of airfoil sections, or turbomachinery blading, however, requires information on boundary-layer development in a pressure gradient. The need for information is usually most acute for the suction surface of such airfoils, where most of the boundary layer is under a severe adverse pressure gradient. In this Note, boundary-layer velocity profiles on a cascade blade are examined in order to determine the effects of freestream turbulence on the law of the wake.

Experimental Details

The experiments were performed in the cascade wind tunnel at the Whittle Laboratory of the Cambridge University Engineering Department. Boundary-layer measurements were taken on the suction surface of a 30.5 cm chord C-4 compressor blade. Further details of the cascade tunnel and blade are given in Ref. 8. An incidence angle of +4 deg was used for all the experiments. Each blade was fitted with a trip wire at the 10% chord position to ensure a turbulent boundary layer over most of the surface.

For each experiment, the Reynolds number based on inlet velocity and blade chord was set to 5×10^5 . Two sizes of turbulence grid could be placed 9 chords upstream of the leading edge of the blade and these produced a freestream turbulence intensity of 3.14% and 5.20% at a measuring position 1.5 chords upstream of the blade leading edge. A third condition was taken with no grid in place, yielding a turbulence intensity of 0.68% at the measuring station. The pressure gradient remained almost constant over most of the suction surface for all three levels of turbulence intensity. The velocity profiles were measured with a linearized DISA constant-temperature, hot-wire anemometer. The correction procedure proposed by Wills⁹ for hot-wire readings close to a wall were used for the first few points near the blade surface.

Coles' Profile Fits

The velocity profile for turbulent boundary layers described by Coles¹⁰ has received widespread acceptance for low-turbulence flows. The complete profile is given by

$$\frac{U}{u_\tau} = \frac{1}{K} \ln \left(\frac{yu_\tau}{\nu} \right) + C + \frac{\Pi}{K} w \left(\frac{y}{\delta} \right) \quad (1)$$

where $w(y/\delta)$ is the wake function which Coles¹¹ has given as

$$w \left(\frac{y}{\delta} \right) = 2 \sin^2 \left(\frac{\Pi}{2} \frac{y}{\delta} \right) \quad (2)$$

The constants K and C in the law of the wall are usually taken as 0.41 and 5.0, respectively. In this Note, a number of experimental velocity profiles are examined, at three different levels of freestream turbulence, to determine the effect of freestream turbulence on the law of the wake. Semilogarithmic velocity profiles at the 80% chord position are shown in Fig. 1 for the three levels of freestream turbulence. There is seen to be a distinct decrease in the wake component with increasing levels of freestream turbulence, which can be explained by the increased fullness of the outer profiles due to increased mixing with the turbulent freestream.

The first step in this investigation was to see if all of the data obtained in the outer layer could be fit to the Coles profiles. Figure 2 shows the results of plotting the data at the 80% chord position in the form of the Coles wake function $w(y/\delta)$ determined from

$$w \left(\frac{y}{\delta} \right) = \left\{ \frac{U}{u_\tau} - \left(\frac{1}{K} \ln \frac{yu_\tau}{\nu} + C \right) \right\} \frac{\Pi}{K}$$

as a function of y/δ . For each profile, the values for Π and u_τ have been obtained from the fitting procedure proposed by Coles.¹¹ It can be seen that the data collapse quite well onto Coles' analytical wake function. A similar collapse of the data at the 50 and 70% chord positions was found, but the fit to the analytical wake function was not quite as good, possibly due to the relatively small wake component in these profiles. The conclusion can be drawn from Fig. 2 that, at least for the limited data obtained, the law of the wake has

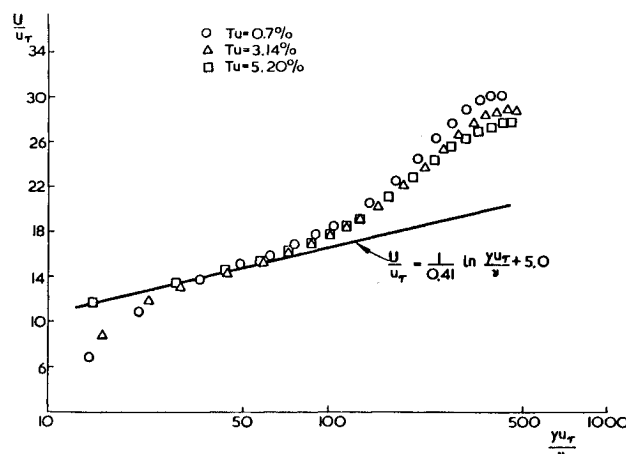


Fig. 1 Semilogarithmic velocity profiles, $X/C = 0.8$.

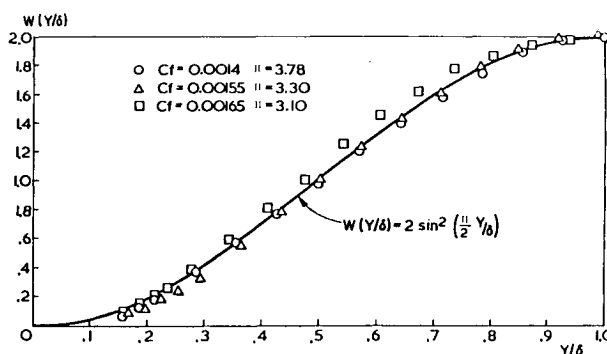


Fig. 2 Coles' wake component, $X/C = 0.8$.

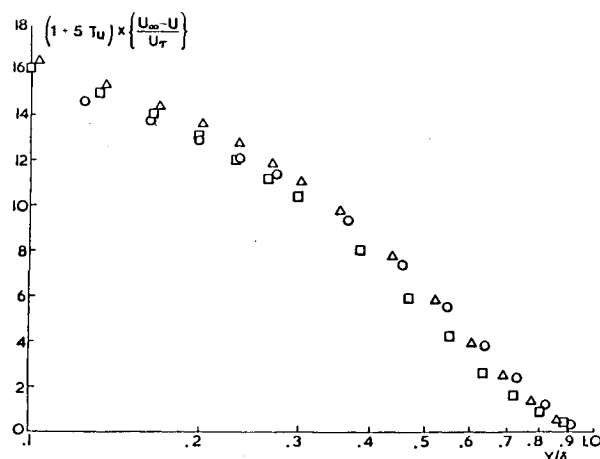


Fig. 3 Modified velocity defect profiles, $X/C=0.7$.

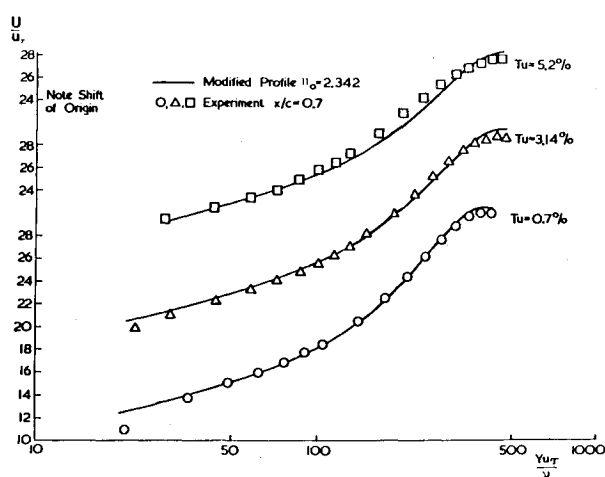


Fig. 4 Coles' profile modified for freestream turbulence.

validity, independent of freestream turbulence, as long as Π and u_τ are determined independently for each level of freestream turbulence.

The Law of the Wake Modified for Freestream Turbulence

The next step in the analysis was an examination of the outer layer velocity defect profiles. For boundary layers developing under the same pressure gradient, one might expect the velocity defect profiles at a given position to collapse onto a single curve in the outer layer, provided that the dependence of the profiles on u_τ is slight. With increasing freestream turbulence levels, the velocity defect was found to decrease, as would be expected with the fuller velocity profiles and decreased wake components.

A reasonable collapse of the velocity defect profiles onto a single curve was obtained by multiplying the defect by $(1 + 5Tu)$, as can be seen from Fig. 3. On the basis of the limited data from the present experiments, the correlation

$$(1 + 5Tu) \frac{U_\infty - U}{u_\tau} = f \left[\log \left(\frac{y}{\delta} \right) \right]$$

is suggested for boundary layers developing under the same adverse pressure gradient, but with varying levels of freestream turbulence. The velocity defect profile collapses quite

well using this correlation for all the profiles measured here, as well as for the zero pressure gradient data of Evans.³ However, further experimental evidence needs to be obtained before this correlation can be confirmed for all pressure gradients and turbulence levels.

A modified form of the Coles profile may therefore be proposed for boundary layers developing in a turbulent freestream. The modified form of the profile is

$$\frac{U}{u_\tau} = \frac{1}{K} \ln \left(\frac{yu_\tau}{\nu} \right) + C + (1 - 5Tu) \frac{\Pi_0}{K} w \left(\frac{y}{\delta} \right)$$

where Π_0 is the wake parameter for the boundary layer developing under the same pressure gradient, but with $Tu=0$. Figure 4 shows the modified profile used to describe the data at three freestream turbulence levels at the 70% chord position. All profiles have used the value of $\Pi_0 = 2.342$, which was obtained by extrapolating the data to $Tu=0$. It can be seen that the modified profile gives a quite reasonable description of the data, even though the wake component changes substantially with increasing levels of freestream turbulence.

Conclusions and Recommendations

The Coles profile for turbulent boundary layers has been shown to be valid for an adverse pressure gradient boundary layer developing under a turbulent freestream. A reasonable collapse of the outer layer velocity defect profiles was found by multiplying the nondimensional defect by $(1 + 5Tu)$. A modified form of the Coles velocity profile has been proposed that appears to be valid for varying levels of freestream turbulence less than about 5%, at least for the pressure gradient used in these experiments. In order to further validate the proposed profile, however, a systematic study of the effects of varying freestream turbulence level and pressure gradient should be conducted.

References

- Kline, S. J., Lisin, A. V., and Waitman, B. A., "Preliminary Experimental Investigation of Effect of Free Stream Turbulence on Turbulent Boundary Layer Growth," NASA TN D-368, 1960.
- Charnay, G., Comte-Bellot, G., and Mathieu, J., "Development of a Turbulent Boundary Layer on a Flat Plate in an External Turbulent Flow," AGARD CP 93, 1972, pp. 27.1-27.10.
- Evans, R. L., "Free-Stream Turbulence Effects on the Turbulent Boundary Layer," British Aeronautical Research Council, CP 1282, 1974.
- Hancock, P. E., and Bradshaw, P., "The Effect of Free-Stream Turbulence on Turbulent Boundary Layers," *ASME Journal of Fluids Engineering*, Vol. 105, Sept. 1983, pp. 284-289.
- Meir, H. U. and Kreplin, H. P., "Influence of Free-Stream Turbulence on Boundary Layer Development," *AIAA Journal*, Vol. 18, Jan. 1980, pp. 11-15.
- Raghunathan, S. and McAdam, R.J.W., "Freestream Turbulence Effects on Attached Subsonic Turbulent Boundary Layers," *AIAA Journal*, Vol. 21, April 1983, pp. 503-508.
- Hancock, P. E., "The Effect of Free Stream Turbulence on Turbulent Boundary Layers," Ph.D. Thesis, Imperial College, London, 1980.
- Evans, R. L., "The Effects of Freestream Turbulence on the Profile Boundary Layer and Losses in a Compressor Cascade," ASME Paper 84-GT-242, 1984.
- Wills, J.A.B., "The Correction of Hot-Wire Readings for Proximity to a Solid Boundary," *Journal of Fluid Mechanics*, Vol. 12, March 1962, pp. 388-396.
- Coles, D., "The Law of the Wake in the Turbulent Boundary Layer," *Journal of Fluid Mechanics*, Vol. 1, July 1956, pp. 191-226.
- Coles, D., "The Young Persons Guide to the Data," *Proceedings, AFOSR-IFP-Stanford Conference on Turbulent Boundary Layers*, Vol. 2, 1968, pp. 1-45.